CRITICAL POINTS IN THE NOISEBERG ACHIEVABLE REGION OF THE GAUSSIAN Z-INTERFERENCE CHANNEL

MAX COSTA (UNICAMP), CHANDRA NAIR (CUHK), AND DAVID NG (CUHK)

ABSTRACT. The Gaussian signaling strategy with power control for the Gaussian Z-interference channel with weak interference is reviewed in this paper. In particular, we study the various communication strategies that may arise at various points of the capacity region and identify the locations of the phase transitions between the various strategies. The Gaussian Z-interference channel with weak interference is known to have two critical points in its capacity region, where the slope of the region shows a sudden change. They occur at the points of the unconditional maximum rate for one of the users and the maximum rate that can be accommodated by the other user. In this paper, we discuss additional critical points (locations of phase transitions) in the achievable region of this channel. These turn out to be second-order phase transitions, i.e., we do not observe a discontinuous slope in the achievable rate region, but there is a discontinuity in the second derivative of the rate contour of the achievable region. This review paper is mainly based on some of our ITA (Information Theory and Applications Workshop, UCSD, San Diego, CA, USA) papers since 2011.

1. INTRODUCTION

Many authors have studied scalar Gaussian interference channels since 1974 [1–32]. One of the key questions in this area, for which we do not have a definitive answer as yet, is whether Han–Kobayashi inner bound with Gaussian signaling achieves the capacity region.

The model under investigation in this paper is the one-sided interference channel given by $Y_1' = X_1' + Z_1'$ and $Y_2' = X_2' + aX_1' + Z_2'$, where X_1' and X_2' are transmitter signals constrained to have average powers Q_1 and Q_2, respectively, a is an interference gain in the interval $(0,1)$, Z_1' and Z_2' are Gaussian noises of unit variance, and Y_1' and Y_2' are the two received signals. This model is depicted in Figure 1.
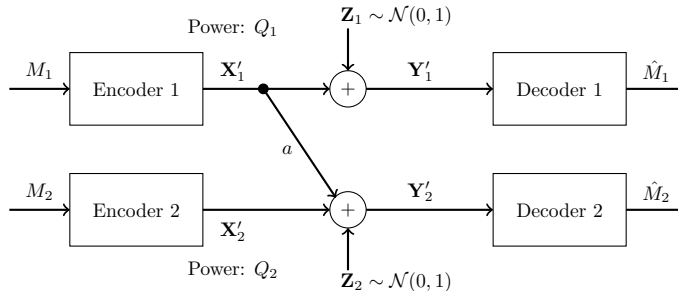

FIGURE 1. Gaussian Z-Interference Channel.

The receivers are interested in messages sent by their respective, same-indexed, transmitters. Thus X_1' encodes a message addressed to receiver 1 and X_2' conveys a message to receiver 2. This model is a particular case of the Gaussian interference channel, which exhibits interference in both directions. Like in the more general model, the problem of finding the associated capacity region has been open for almost 50 years. In the case of strong interference, when $a \geq 1$, the capacity region is known [19,31]. In this case, the unintended receiver can fully decode the interfering message. Therefore, the rate region coincides with the intersection of the two underlying multiple access channel regions. Also, when $a = 0$, the problem has a trivial solution. This paper uses the fact that the Gaussian Z-interference channel with interference parameter a in the range $(0,1)$ can be regarded as a degraded Gaussian interference channel [6], a model shown in Figure 2.
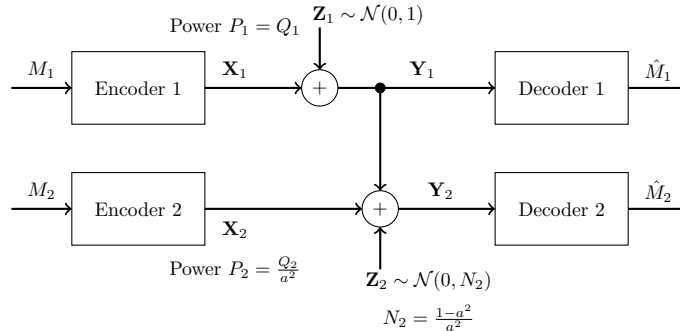
FIGURE 2. Degraded Gaussian Interference Channel.

Like the Gaussian Z-interference channel, the degraded Gaussian interference channel is characterized by three parameters: the two powers P_1 and P_2, and the additional independent noise in the second receiver, power N_2. These parameters are related to the parameters of the original Z-interference channel by $P_1 = Q_1$, $P_2 = Q_2/a^2$ and $N_2 = (1 - a^2)/a^2$. Moreover, since $0 < a < 1$, the additional noise power N_2 is always positive. For simplicity, we choose to use the more common notation, without the primes, in this channel, which will constitute our working model.

In this review paper, we investigate the behavior of the noiseberg encoding scheme [7], which has recently been shown [9] to coincide with the Han–Kobayashi region with Gaussian signaling. From a communication engineer's perspective, knowing the optimal Gaussian signaling strategy for a given set of parameters is essential when maximizing $R_1 + \beta R_2$. In particular, we investigate additional critical points in the achievable region of the noiseberg scheme for the Gaussian Z-interference channel with weak interference. These critical points are associated with transitions between different modes of operation. A third critical point happens between the so-called multiplex and the overflow regions produced in the noiseberg encoding scheme [7]. A fourth critical point happens after the overflow mode is in effect, as the evolution of modes leads to a transition to pure superposition or, otherwise, reaches an extreme boundary in the λ x h parameter space.

Another possible transition may happen when the noiseberg region takes up all the power available for P_1 before the noiseberg height reaches the overflow level (N_2). This will be characterized as a transition from Phase 4 to Phase 7. Subsequently, the optimal path in this case will transition to Phase 6 and, finally, to Phase 3.

2. PRELIMINARIES

We focus on the degraded interference channel model depicted in Figure 2. Two extreme points in the channel capacity region have been identified for this channel. One extreme point occurs when X_1 sends information at its maximum possible rate and X_2 uses what is left of the channel, with X_1's interference treated as noise. In this extreme point the achieved rate pair (R_1, R_2) is given by $R_1 = \frac{1}{2}\log(1 + P_1)$ and $R_2 = \frac{1}{2}\log(1 + \frac{P_2}{1 + P_1 + N_2})$ (cf. Figure 3). There is a slope discontinuity for the capacity region at this extreme point, which follows from the capacity region of an associated degraded broadcast channel [6,30], establishing that this extreme point is a critical point. From this, it immediately follows that this point also maximizes $R_1 + R_2$, the sum-rate, and therefore, this corner point will be referred to as the sum-rate corner point.

Another extreme point in the achievable region occurs when all the privilege of operating at maximum rate is given to the second transmitter [6,26]. In this case, the first transmitter must lower its rate to the point where the second receiver is sure to decode and eliminate all the interference that its signaling might impose. The first transmitter then uses the noisy channel that sees noise power $1 + N_2 + P_2$. Therefore, we have $R_1 = \frac{1}{2}\log(1 + \frac{P_1}{1 + N_2 + P_2})$ and $R_2 = \frac{1}{2}\log(1 + \frac{P_2}{1 + N_2})$. There is also a slope discontinuity for the capacity region at this extreme point, which follows from a recent outer bound developed in [16]. This corner point is referred to as the back-off corner point.
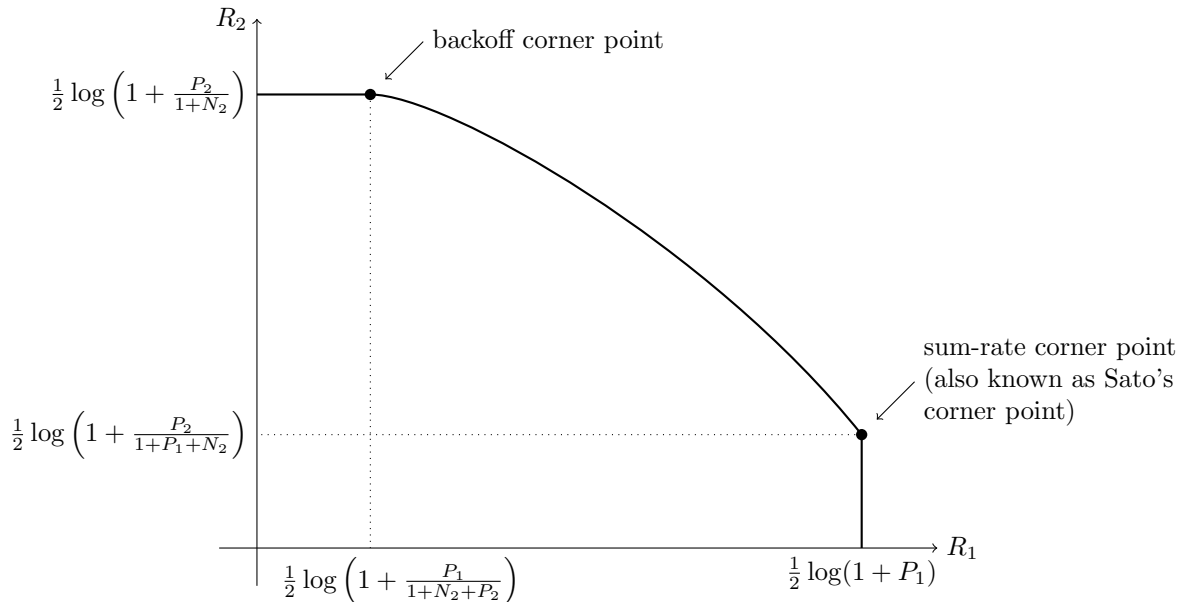
FIGURE 3. Critical points of the capacity region.

2.1. **Noisebergs – a Brief Review.** A noiseberg transmission scheme is a particular Gaussian signaling strategy with power control, with (only) seven potential phases, depicted in Figures 4, 5, 6, 7, 8, 9, and 10. In a nutshell, it is a scheme that combines superposition coding, non-naïve (i.e., power-controlled) time-sharing, and water filling between the two spectral regions that get multiplexed. More specifically, it is a time-sharing/bandwidth-sharing between two signaling strategies, with the first strategy (depicted on the left) occupying $(1-\lambda)$ fraction of the time (band) and the second strategy occupying the remaining λ fraction of the time (band). In particular, the strategies in Figures 4, 5, and 6 can be considered as special instances of those in Figure 7, 8, and 9 respectively by setting $\lambda = 0$. In the leftmost strategy, using band $(1 - \lambda)$, one allocates part of the power budget to combine transmissions to both decoders in a pure superposition manner, exactly as is known to be optimal for Gaussian broadcast channels. In the second strategy, over band λ, the communication is solely accomplished between the first transmitter and the first receiver. Yet, this strategy can also be interpreted as a particular point of the capacity region of a Gaussian broadcast channel, restricted to maximal R_1 and null R_2.

Consider the following seven communication strategies, using Gaussian signaling, for the Gaussian interference channel:

(1) Phase 1: *Treating interference to be noise at the weaker receiver (Sato's corner point)*

In this phase, the weaker receiver, Y_2, decodes its message by treating X_1 as noise. This is depicted pictorially in Figure 4. The decoding order in the picture is assumed to go from top to bottom. Any receiver will decode all the messages on top of its message (including its message) in any band by treating those below it as noise. The rate pair achieved in this phase is

$$R_1 = \frac{1}{2} \log \left(1 + P_1\right), R_2 = \frac{1}{2} \log \left(1 + \frac{P_2}{1 + P_1 + N_2}\right).$$
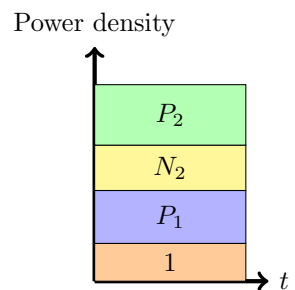
Power density

FIGURE 4. Phase 1 (Sato's corner point).

(2) Phase 2: *Partial interference cancellation at the weaker receiver (or pure superposition coding)*

Power density

In this phase, the weaker receiver, Y_2, decodes a part of X_1 first, subtracts this from the received signal, and then decodes its own signal X_2. The rate pair achieved in this phase is

$$R_1 = \frac{1}{2} \log \left(1 + \frac{P_{1C}}{1 + N_2 + P_2 + P_{1A}} \right) + \frac{1}{2} \log \left(1 + P_{1A} \right),$$

$$R_2 = \frac{1}{2} \log \left(1 + \frac{P_2}{1 + N_2 + P_{1A}} \right).$$

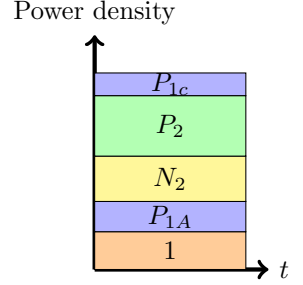Note that $P_{1A} + P_{1C} = P_1$. This can be seen as a mix of Phase 1 and Phase 3, to be seen next.

FIGURE 5. Phase 2 (Pure superposition strategy).

(3) Phase 3: *Interference cancellation at the weaker receiver (the backoff corner point)*

Power density

In this phase, the weaker receiver, Y_2, decodes X_1 first, subtracts this from the received signal, and finally decodes its own signal X_2. The rate pair achieved in this phase is

$$R_1 = \frac{1}{2} \log \left(1 + \frac{P_1}{1 + N_2 + P_2} \right), R_2 = \frac{1}{2} \log \left(1 + \frac{P_2}{1 + N_2} \right).$$

Note that the rate for message 1 is solely determined by the ability of the weaker decoder to decode it. This encoding strategy is similar to that in a degraded message sets Gaussian broadcast channel where message 1 is meant to be communicated to both receivers.
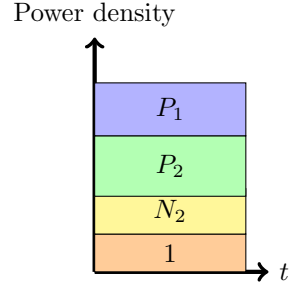

FIGURE 6. Phase 3 (Backoff corner point).

(4) Phase 4: *Time-sharing between the following two strategies: Treating interference to be noise at the weaker receiver and transmitting solely to the stronger receiver (or multiplex strategy)*

In this phase, there is a time-sharing between two communication schemes. The first scheme, employed for $(1 - \lambda)$ fraction of the time, employs the Phase 1 strategy, and the second scheme consists of transmission only to the stronger receiver. The total average power in each band is indicated in the figure. Therefore, one must divide the power by the band duration to get the height. It is this phase that leads to the noiseberg nomenclature. We denote by h, the height difference between the N_2 slab in the second band and the power level of P_2 in the first band. This height difference comes from part of the noise spectrum of Z_2 that floats above the signal level in the first band and characterizes what we call a noise-iceberg, or *noiseberg*. The flotation of the noise slab releases prime-rate space in the power $\times$ bandwidth plane, in a fashion that Archimedes would be sure to appreciate. In this phase, we get the following:

$$P_1 = P_{1A} + P_{1B}$$
$$\frac{P_{1A} + P_2}{1 - \lambda} = \frac{P_{1B}}{\lambda} - h. \tag{1}$$

The rate pairs achieved in this scheme are

$$R_1 = \frac{\bar{\lambda}}{2} \log \left(1 + \frac{\bar{\lambda} P_1 - \lambda \bar{\lambda} h - \lambda P_2}{\bar{\lambda}} \right) + \frac{\lambda}{2} \log \left(1 + P_1 + P_2 + \bar{\lambda} h \right),$$

$$R_2 = \frac{\bar{\lambda}}{2} \log \left(1 + \frac{P_2}{\bar{\lambda}(1 + N_2) + \bar{\lambda} P_1 - \lambda \bar{\lambda} h - \lambda P_2} \right), \tag{2}$$

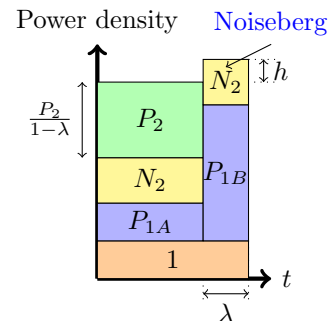where $\bar{\lambda}$ denotes $(1 - \lambda)$.

Power density   Noiseberg

FIGURE 7. Phase 4 (The noiseberg strategy).

(5) Phase 5: *Time-sharing between the following two strategies: Partial interference cancellation at the weaker receiver and transmitting solely to the stronger receiver (or overflow strategy)*

In this phase, as before, there is a time-sharing between two communication schemes. The first scheme, employed for $(1 - \lambda)$ fraction of the time, employs the Phase 2 strategy, and the second scheme consists of transmission only to the stronger receiver. The total average power in each band is indicated in the figure. We denote by h, the height difference between the top of the N_2 slab in the second band and the power level of P_2 in the first band. Again, as argued in [7, 9], the total heights of the two signal bands must agree via a water-filling argument. The noise band of height N_2 floats above the signal power band in the rightmost strategy. The floating of the noise band frees up prime frequency (or time) space in the spectrum for signal occupation.

In this phase, we get the following:

$$P_1 = P_{1A} + P_{1B} + P_{1C}$$

$$\frac{P_{1B}}{\lambda} = N_2 + \frac{P_2 + P_{1A} + P_{1C}}{\bar{\lambda}} \tag{3}$$

$$\frac{P_{1C}}{1 - \lambda} = h - N_2$$

$$
\begin{aligned}
R_1 = {}& \frac{\bar{\lambda}}{2} \log \left(1 + \frac{\bar{\lambda}P_1 - \lambda P_2 - \bar{\lambda}h + \bar{\lambda}^2 N_2}{\bar{\lambda}} \right) \\
&+ \frac{\bar{\lambda}}{2} \log \left(1 + \frac{\bar{\lambda}(h - N_2)}{\bar{\lambda}(1 + N_2) + \bar{\lambda}P_1 - \lambda P_2 - \bar{\lambda}h + \bar{\lambda}^2 N_2 + P_2} \right) \\
&+ \frac{\lambda}{2} \log \left(1 + P_1 + P_2 + \bar{\lambda}N_2 \right),
\end{aligned}
\tag{4}
$$

$$R_2 = \frac{\bar{\lambda}}{2} \log \left(1 + \frac{P_2}{\bar{\lambda}(1 + N_2) + \bar{\lambda}P_1 - \lambda P_2 - \bar{\lambda}h + \bar{\lambda}^2 N_2} \right).$$

FIGURE 8. Phase 5 (The overflow region).

(6) Phase 6: *Time-sharing between the following two strategies: Interference cancellation at the weaker receiver and transmitting solely to the stronger receiver (top boundary of the admissible parameter region)*

In this phase, there is also a time-sharing between two communication schemes. The first scheme, employed for $(1 - \lambda)$ fraction of the time, employs the Phase 3 strategy, and the second scheme consists of transmission only to the stronger receiver. The total average power in each band is indicated in the figure. As in Phase 5, we denote by h, the height difference between the top of the N_2 slab in the second band and the power level of P_2 in the first band. As argued in [7, 9], the total heights of the two bands must agree via a water-filling argument.

In this phase, we get the following:

$$P_1 = P_{1C} + P_{1B}$$

$$\frac{P_{1B}}{\lambda} = N_2 + \frac{P_2 + P_{1C}}{\bar{\lambda}} \tag{5}$$

$$\frac{P_{1C}}{1 - \lambda} = h - N_2$$

$$
\begin{aligned}
R_1 = {}& \frac{\bar{\lambda}}{2} \log \left(1 + \frac{\bar{\lambda}P_1 - \lambda\bar{\lambda}N_2 - \lambda P_2}{\bar{\lambda}(1 + N_2) + P_2} \right) \\
&+ \frac{\lambda}{2} \log \left(1 + P_1 + P_2 + \bar{\lambda}N_2 \right),
\end{aligned}
$$
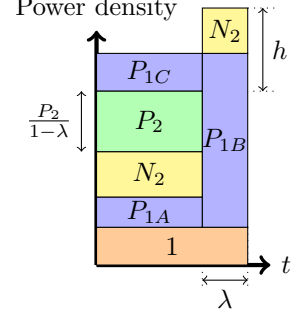
$$R_2 = \frac{\bar{\lambda}}{2} \log \left(1 + \frac{P_2}{\bar{\lambda}(1 + N_2)} \right).$$
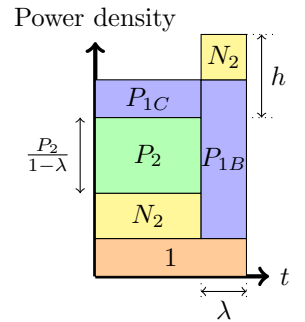

FIGURE 9. Phase 6 (The top boundary of the admissible (λ, h) parameter region).

(7) Phase 7: *Time-division between transmitting solely to the two receivers*

In this phase, for $(1 - \lambda)$ fraction of the time, we transmit solely to the weaker receiver, and for λ fraction of the time, we transmit solely to the stronger receiver. In this phase, we obtain

$$R_1 = \frac{\lambda}{2} \log\left(1 + \frac{P_1}{\lambda}\right),$$

$$R_2 = \frac{\bar{\lambda}}{2} \log\left(1 + \frac{P_2}{\bar{\lambda}(1 + N_2)}\right).$$
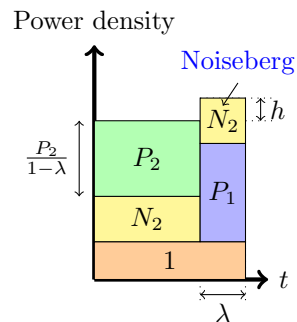
FIGURE 10. Phase 7 (Essentially, a portion of the so called non-naive time sharing).

Remark 1. *A general Gaussian signaling strategy incorporating superposition coding and non-naïve (i.e., power-controlled) time-sharing will have many more phases than those described above. However, it was proposed in [7] and established in [9] that the boundary of the Gaussian signaling region is obtained by restricting to these seven strategies.*

2.2. **The Gaussian Signaling Region.** One needs to optimize $R_1 + \beta R_2$ for $1 \leq \beta \leq \infty$, among the various signaling strategies or phases to compute the Gaussian signaling region.

2.2.1. *Slopes at the Corner Points.* It is known [6, 31] that $R_1 + R_2$ (i.e. $\beta = 1$) is maximized (for the capacity region) at the corner point $R_1 = \frac{1}{2} \log(1 + P_1)$ and $R_2 = \frac{1}{2} \log\left(1 + \frac{P_2}{1 + N_2 + P_1}\right)$. Note that $R_1 + \beta R_2$ for $0 \leq \beta \leq 1$ will also pass through the same corner point, as this corresponds to the maximum value of R_1. This corresponds to a Phase 1 communication strategy. In particular, it has been shown [13] that the supporting hyperplane, $R_1 + \beta R_2$, will touch the Gaussian signaling region (or equivalently the noiseberg region) at the same corner point if and only if $\beta \leq \beta_{Sato}$ (defined below). Thus, β_{Sato} marks the first critical (or phase-transition) point of the noiseberg region.

Theorem 1 ([13])**.** *For a Gaussian Z-interference channel, let β_{Sato} be the largest value of $\beta \geq 1$ such that*

$$\sup_{(R_1, R_2) \in \mathcal{R}^{HK\text{-}GS}} (R_1 + \beta R_2) = \frac{1}{2} \log(1 + P_1) + \frac{\lambda}{2} \log\left(1 + \frac{P_2}{1 + N_2 + P_1}\right). \tag{6}$$

Then

$$\beta_{Sato} = \min\left\{\frac{(N_2 + P_2)(1 + N_2 + P_1)}{P_2(1 + P_1)}, \beta^*\right\},$$

where β^* is the unique positive solution $\psi(\beta) = 0$, where

$$\psi(\beta) := \beta \left(\log\left(1 + \frac{P_2}{1 + N_2 + P_1}\right) - \frac{N_2 P_2}{(1 + N_2 + P_1)(1 + N_2 + P_1 + P_2)}\right)$$

$$+ \log\left(1 - \frac{P_2(1 + P_1)}{(1 + N_2 + P_1)(1 + N_2 + P_1 + P_2)}\beta\right).$$

Remark 2. *We do not yet have a matching converse (i.e. one that follows from an outer bound to the capacity region) that establishes the slope at this corner point. An interested reader may refer to [16] and [18] for recent developments along these lines.*

On the other hand, it is known that for large enough β the supporting hyperplanes to the Gaussian signaling region, [12], as well as the one to the capacity region [16] pass through the backoff corner point

established in [26], namely $R_1 = \frac{1}{2}\log\left(1 + \frac{P_1}{1+N_2+P_2}\right)$ and $R_2 = \frac{1}{2}\log\left(1+P_2\right)$. This corresponds to a Phase 3 communication strategy. (At this corner point, R_2 takes its maximum value.)

Theorem 2 ([12]). *Consider a Gaussian Z-interference channel. The smallest β such that the supporting hyperplane of the form $R_1 + \beta R_2$ of the Han-Kobayashi signaling scheme with Gaussian inputs passes through the backoff corner point is given by*

$$\beta_{backoff} = 1 + \max\left\{\frac{N_2(1+N_2+P_2)}{P_2}, \frac{\log(1+N_2) - \frac{N_2}{(1+N_2+P_1+P_2)}}{\log\left(\frac{1+P_2+N_2}{1+N_2}\right) - \frac{P_2}{1+P_2+N_2}}\right\}.$$

Thus, for all $\beta \geq \beta_{backoff}$, the supporting hyperplane to the Gaussian signaling region (or the noiseberg region) passes through the above corner point.

Remark 3. *As with the sum-rate point, we do not yet have a matching converse (i.e. one that follows from an outer bound to the capacity region) that establishes the slope at this corner point. An interested reader may refer to [9, 16], where upper bounds on the slope have been established. The issue of corner points to the capacity region of two-user Gaussian interference channels in various signal-to-noise ratio regimes has been studied in [28].*

2.2.2. *The Intermediate Regime, $\beta : \beta_{Sato} \leq \beta \leq \beta_{backoff}$.* The main objective of this paper would be to review the known results for β in the regime $\beta : \beta_{Sato} \leq \beta \leq \beta_{backoff}$. Initially, consider the leftmost (pure superposition coding) strategy, i.e., we only consider Phases 1,2 and 3. In Phase 2, we need to compute

$$\max_{0 \leq P_{1A} \leq P_1} \frac{1}{2}\log\left(1 + \frac{P_1 - P_{1A}}{1+N_2+P_2+P_{1A}}\right) + \frac{1}{2}\log\left(1+P_{1A}\right) + \frac{\beta}{2}\log\left(1 + \frac{P_2}{1+N_2+P_{1A}}\right).$$

A little bit of calculus shows that optimizing

$$P_{1A} = \begin{cases} P_1 & \text{if } \beta \leq \frac{P_2+N_2}{P_2}\frac{1+P_1+N_2}{1+P_1}, & \text{(Phase 1)} \\ 0 & \text{if } \beta \geq \frac{P_2+N_2}{P_2}(1+N_2), & \text{(Phase 3)} \\ \frac{(1+N_2)(P_2+N_2)-\beta P_2}{\beta P_2 - (P_2+N_2)} & \text{otherwise.} & \text{(Phase 2)} \end{cases}$$

In the above optimization problem, we observe that there are two transition values for β, defined by $\beta_1 = \frac{P_2+N_2}{P_2}\frac{1+P_1+N_2}{1+P_1}$ (marking the transition from Phase 1 to Phase 2) and $\beta_2 = \frac{P_2+N_2}{P_2}(1+N_2)$ (marking the transition from Phase 2 to Phase 3). Note that β_1 corresponds to the first of the two terms in the minimization that defines β_{Sato}, and β_2 corresponds to the first of the two terms in the maximization that defines $\beta_{backoff}$.

It turns out that the second of the two terms in the minimization that defines β_{Sato} corresponds to a phase transition from Phase 1 to Phase 4. Similarly, the second of the two terms in the maximization that defines $\beta_{backoff}$ corresponds to a phase transition from Phase 6 to Phase 3.

Phases 1, 2, and 3 can be considered special instances of Phases 4, 5, and 6, respectively, by setting $\lambda = 0$. Phase 1 (Sato's corner point) is associated with the segment $\lambda = 0$ and $0 \leq h \leq N_2$. Phase 2 (the pure superposition phase) is related to the middle segment formed by $\lambda = 0$ and $N_2 \leq h \leq N_2 + P_1$. Finally, Phase 3 (the backoff corner point) is mapped to the single point, $\lambda = 0$, and $h = N_2 + P_1$.

Further, the rate pairs (R_1, R_2) in Phases 4, 5, and 6 can also be expressed in terms of the parameters λ and h as stated before. These parameters λ, h vary over a region, called the region of admissible points, defined by the conditions that P_{1A}, P_{1B}, and P_{1C} are non-negative and sum to P_1. The region $h \leq N_2$ and $\lambda > 0$ corresponds to Phase 4. If $h \geq N_2$, then $P_{1C} > 0$, and this is called the overflow region. This encompasses Phases 5 and 6.

The admissible region in Phase 4, using (1), can be shown to be restricted by the expressions $0 \leq h \leq N_2$ and

$$0 < \lambda \leq \frac{P_1 + P_2 + h - \sqrt{(P_1+P_2+h)^2 - 4P_1 h}}{2h}.$$

The admissible region in Phase 5, using (3), can be shown to be restricted by the expressions $N_2 < h \leq N_2 + P_1$ and

$$0 < \lambda < \frac{P_1 + P_2 + 2N_2 - h - \sqrt{(P_1+P_2+2N_2-h)^2 - 4N_2(P_1+N_2-h)}}{2N_2}.$$

Finally, the admissible region in Phase 6, using (5), can be shown to be restricted by the expressions $N_2 < h \le N_2 + P_1$ and

$$\lambda = \frac{P_1 + P_2 + 2N_2 - h - \sqrt{(P_1 + P_2 + 2N_2 - h)^2 - 4N_2(P_1 + N_2 - h)}}{2N_2}.$$

Figure 11 shows the admissible region of λ and h for the parameters $P_1 = 1, P_2 = 4, N_2 = 3$. Phases 1, 2, and 3 correspond to $\lambda = 0$ and collapse to Y-axis. Phase 6 corresponds to the upper boundary. The dotted line at $h = 3$ marks the phase boundary between Phases 4 (noiseberg multiplex) and 5 (overflow). Finally, Phase 7 is the rightmost boundary of the admissible region, that is reached in case the boundary is met before overflow.
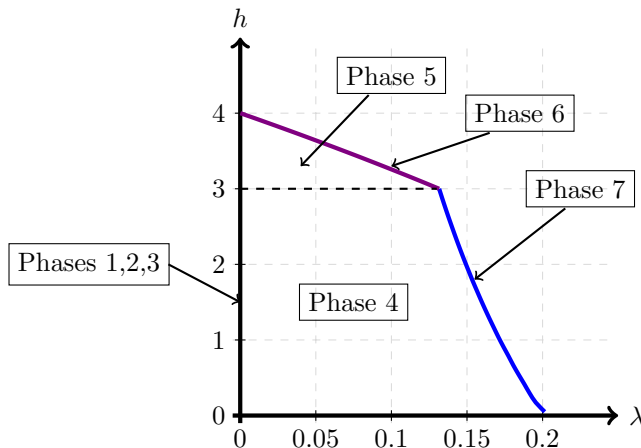

FIGURE 11. Contour of admissible region for a Z-interference channel with $Q_1 = 1$, $Q_2 = 1$, $a = 0.5$, i.e. a degraded channel with $P_1 = 1$, $P_2 = 4$, $N_2 = 3$.

To determine the phase, we need to maximize $R_1(h, \lambda) + \beta R_2(h, \lambda)$ (using (2) or (4) depending on $h \le N_2$ or $h \ge N_2$, respectively) and this leads to a path of optimal extreme points in the admissible region.

Apart from the phase transitions characterized in Theorems 1 and 2, namely, Phase 1 → Phase 2, Phase 1 → Phase 4, Phase 2 → Phase 3, and Phase 6 → Phase 3, the numerical experiments show that there are five more types of phase transitions in the Gaussian signaling scheme. These other ones represent the transitions from Phase 4 → Phase 5, Phase 4 → Phase 7, Phase 7 → Phase 6, Phase 5 → Phase 2, and Phase 5 → Phase 6, and let us define the corresponding β's to be $\beta_{4 \to 5}$, $\beta_{4 \to 7}$, $\beta_{5 \to 6}$, $\beta_{5 \to 2}$, and $\beta_{5 \to 6}$ respectively. These phase transitions can be implicitly characterized as follows:

- $\beta_{4 \to 5}$: This corresponds to the β at which $R_1(h, \lambda) + \beta R_2(h, \lambda)$ is maximized when $h = N_2$ and $\lambda > 0$. This corresponds to the transition between the multiplex and overflow regions.
- $\beta_{4 \to 7}$: This corresponds to the β at which $R_1(h, \lambda) + \beta R_2(h, \lambda)$ is maximized when $h < N_2$ and $\lambda = \frac{P_1 + P_2 + h - \sqrt{(P_1 + P_2 + h)^2 - 4P_1 h}}{2h}$, in other words $P_{1A} = 0$. This corresponds to the transition from the multiplex region to the non-naive time-division region.
- $\beta_{7 \to 6}$: This corresponds to the β at which $R_1(h, \lambda) + \beta R_2(h, \lambda)$ is maximized when $h = N_2$ and $\lambda = \frac{P_1 + P_2 + h - \sqrt{(P_1 + P_2 + h)^2 - 4P_1 h}}{2h}$. This corresponds to the transition from the time-division phase to the overflow region, with $P_{1A} = 0$.
- $\beta_{5 \to 2}$: This corresponds to the β at which $R_1(h, \lambda) + \beta R_2(h, \lambda)$ is maximized when $h > N_2$ and $\lambda = 0$. This corresponds to the transition from the overflow region to a pure superposition coding region.
- $\beta_{5 \to 6}$: This corresponds to the β at which $R_1(h, \lambda) + \beta R_2(h, \lambda)$ is maximized when $h > N_2$ and $\lambda = \frac{P_1 + P_2 + 2N_2 - h - \sqrt{(P_1 + P_2 + 2N_2 - h)^2 - 4N_2(P_1 + N_2 - h)}}{2N_2}$. This corresponds to the transition from the interior of the admissible (h, λ) region to the top boundary of this region.

2.2.3. *Trajectories in the phase space.* In this section, we plot the various trajectories of the optimizing parameters in the phase space of (h, λ) as we vary β from β_{sato} to $\beta_{backoff}$.

(1) **Path 1**: For some set of parameters (for example, $P_1 = 1, P_2 = 9, N_2 = 8$) numerical simulations indicate that the optimal path is Phase 1 → Phase 2 → Phase 3. (This is the path of pure superposition evolution) and the locations of the phase transitions occur at $\beta_{1 \to 2} = 9\frac{4}{9}$ and $\beta_{2 \to 3} = 17$ respectively. This implies that the trajectory in the admissible region is only along the h-axis, i.e., with $\lambda = 0$.

(2) **Path 2**: For some set of parameters (for example, $P_1 = 1, P_2 = 4, N_2 = 1$) the optimal path seems to be Phase 1 → Phase 4 → Phase 5 → Phase 2 → Phase 3. The phase transitions occur at (approximately) $\beta_{1 \to 4} = 1.8422$, $\beta_{4 \to 5} = 1.9549$, $\beta_{5 \to 2} = 2.0799$ and $\beta_{2 \to 3} = 2.5$ respectively. This path is depicted in Figure 12.
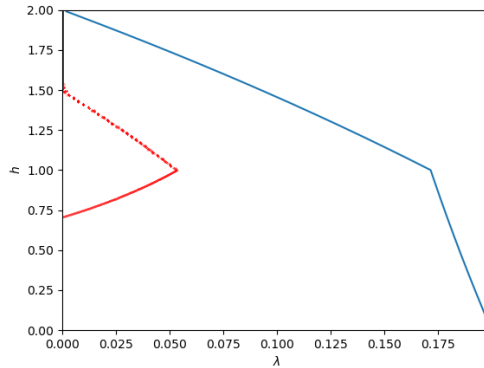

FIGURE 12. Contour of the admissible region and optimized points (obtained numerically) for a Z-interference channel with $Q_1 = 1$, $Q_2 = 2$, $a = \frac{\sqrt{2}}{2}$, i.e. a degraded channel with $P_1 = 1$, $P_2 = 4$, $N_2 = 1$.

As the figure illustrates, it leaves Phase 1 (Sato point) and moves into Phase 4. Then, at $h = N_2 = 1$, it moves from Phase 4 to Phase 5. Then, at $h \approx 1.5$, it moves from Phase 5 to Phase 2. Finally, at $h = 2$, the trajectory reaches the other corner point.

(3) **Path 3**: For some set of parameters (for example $P_1 = 1, P_2 = 2.5, N_2 = 1$) the optimal path seems to be Phase 1 → Phase 4 → Phase 5 → Phase 6 → Phase 3. The phase transitions occur at (approximately) $\beta_{1 \to 4} = 1.9238$, $\beta_{4 \to 5} = 2.4153$, $\beta_{5 \to 6} = 2.6987$, and $\beta_{6 \to 3} = 3.0023$ respectively. This path is depicted in Figure 13.
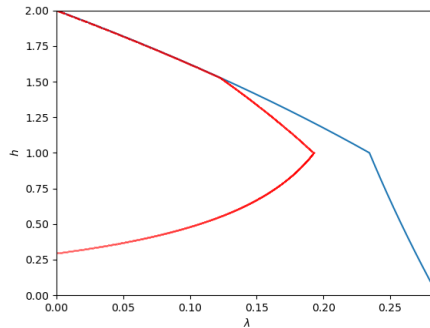

FIGURE 13. Admissible region and optimized points (obtained numerically) for a Z-interference channel with $Q_1 = 1$, $Q_2 = 1.25$, $a = \frac{1}{\sqrt{2}}$, i.e. a degraded channel with $P_1 = 1$, $P_2 = 2.5$, $N_2 = 1$.

As the figure illustrates, it leaves Phase 1 (Sato point) and moves into Phase 4. Then, at $h = N_2 = 1$, it moves from Phase 4 to Phase 5. At a slightly larger β, it enters Phase 6 and remains there until it reaches the new corner point at Phase 3.

(4) **Path 4**: For some set of parameters (for example $P_1 = 1, P_2 = 1, N_2 = 3$) the optimal path seems to be Phase 1 $\rightarrow$ Phase 4 $\rightarrow$ Phase 7 $\rightarrow$ Phase 6 $\rightarrow$ Phase 3. The phase transitions occur at (approximately) $\beta_{1 \rightarrow 4} = 5.3182$, $\beta_{4 \rightarrow 7} = 9.5662$, $\beta_{7 \rightarrow 6} = 23.3434$, and $\beta_{6 \rightarrow 3} = 39.2955$ respectively.
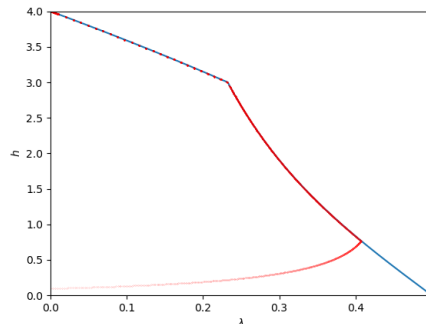
This path is depicted in Figure 14.

FIGURE 14. Admissible region and optimized points (obtained numerically) for a Z-interference channel with $Q_1 = 1$, $Q_2 = 0.25$, $a = \frac{1}{2}$, i.e. a degraded channel with $P_1 = 1$, $P_2 = 1$, $N_2 = 3$.

2.3. **To Mux or Not to Mux.** From the point of view of a converse to the capacity region, it may be helpful to realize that one does not need multiplexing (time-sharing) for some parameters (Q_1, Q_2, a). Hence, there is a potential for the existing techniques for proving the optimality of Gaussian distributions to work.

In Theorem 1, the authors computed the slope, β_{Sato}, of the capacity region at the sum-rate corner point. Whenever the first term there is the critical one, it was observed that the optimal trajectory consists only of the pure superposition phases, i.e., Phases 1, 2, and 3. This leads us to propose the following conjecture.

Conjecture 1. *Consider a degraded Gaussian Z-interference channel with parameters (P_1, P_2, N_2). The noiseberg region consists only of a pure superposition coding strategy (i.e. no time-sharing is required for any β-sum-rate) whenever*

$$\frac{(N_2 + P_2)(1 + N_2 + P_1)}{P_2(1 + P_1)} \leq \beta^*,$$

where β^* is the unique positive solution of $\psi(\beta) = 0$, where

$$\psi(\beta) := \beta \left(\log \left(1 + \frac{P_2}{1 + N_2 + P_1} \right) - \frac{N_2 P_2}{(1 + N_2 + P_1)(1 + N_2 + P_1 + P_2)} \right)$$
$$+ \log \left(1 - \frac{P_2(1 + P_1)}{(1 + N_2 + P_1)(1 + N_2 + P_1 + P_2)} \beta \right).$$

This conjecture allows us to identify the regions of parameters Q_1, Q_2, and a where we have optimal rate evolution between the extreme points with pure superposition alone, i.e., without the use of noisebergs. The results are shown in Figure 15.

Q_1	Q_2	Superposition	Multiplex
1	1	$a < 0.403$	$a > 0.404$
1	> 4.35	$a \in (0, 1)$	never
10	1	$a < 0.1673$	$a > 0.1674$
10	10	$a < 0.637$	$a > 0.638$

FIGURE 15. Boundaries between pure superposition and multiplex regions for different values of Q_1 and Q_2.

2.4. **The other critical points.** Figure 16 depicts the achievable rate region for the parameters $P_1 = 1, P_2 = 2.5, N_2 = 1$. Clearly, the rate region depicts a discontinuity in the slope at the sum-rate extreme point as well as the back-off extreme point. Even the capacity region has been shown to exhibit this behavior. However, in an earlier section (cf. Fig. 13), we claimed that this set of parameters also exhibits a phase transition at (approximately) $\beta_{4\to5} = 2.415$, where the rates are (approximately) $R_1 = 0.238$, $R_2 = 0.353$; and at (approximately) $\beta_{5\to6} = 2.699$, where the rates are (approximately) $R_1 = 0.149$, $R_2 = 0.388$. The achievable rate region does not exhibit a discontinuity in slope at these parameters. However, these are second-order phase transitions of the capacity region, i.e., the second derivative has a discontinuity. This happens because there is a crossing of the curves of β that correspond to two schemes that are involved in the transition. But β is the slope of the normal to the tangent of the achievable rate curve. Therefore the first derivatives of the achievable rate curve will not show a discontinuity at these critical points, but their second derivatives (the slope of the slope) will.
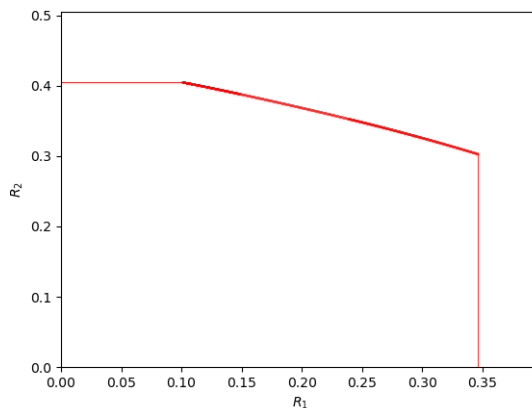

FIGURE 16. The noiseberg achievable region for $P_1 = 1$ $P_2 = 2.5$, and $N_2 = 1$.

For the noiseberg region, the phase transitions $\beta_{4\to7}, \beta_{4\to5}, \beta_{7\to6}, \beta_{5\to6}, \beta_{5\to2}$ all appear to be second-order phase transitions of the capacity region. This is also supported by some back-of-the-envelope calculations, but a formal proof is still absent at this point.

It is rather interesting how the β's arrange themselves to give an achievable rate region with no kinks other than the two corner points. For a general scalar Gaussian interference channel, in a very weak-interference regime, it is known that the capacity region exhibits a kink [3, 24] at the maximum sum-rate point as well. In the Z-interference channel case, the sum-rate point coincides with one of the corner points, perhaps indicating that there are no additional kinks for a general scalar Gaussian interference channel.

3. Conclusion

In this paper, we review new critical points in the noiseberg achievable rate region of the Gaussian Z-interference channel. This region (and the capacity region) has been known to have two critical points at its two corner points. The noiseberg achievable region is observed to have additional points of second-order phase transitions. One of these critical points ($\beta_{4\to5}$) marks the transition of the noiseberg multiplex region into the overflow region. Another of these ($\beta_{4\to7}$) marks the transition of the noiseberg multiplex region into the time-division region. A third critical point ($\beta_{5\to2}$) marks the transition of the overflow region back to the superposition coding region. Finally, a fourth critical point ($\beta_{5\to6}$) marks the transition of the overflow region into a phase where the weaker receiver decodes the interfering signal in its band (Phase 6).

It is hoped that the review of the noiseberg region will help the community resolve the following key open-question: does the noiseberg region coincide with the capacity region of the Gaussian Z-interference channel?

4. Acknowledgement

The authors would like to thank Gustavo Fraidenraich, José Cândido Santos Filho, Dustin Wang, and Amin Gohari for their inspiring discussions. Thanks are also due to the anonymous reviewers for some astute remarks.

References

1. R. Ahlswede, *The capacity region of a channel with two senders and two receivers*, The Annals of Probability **2** (1974), no. 5, 805 – 814.
2. V. Sreekanth Annapureddy and Venugopal V. Veeravalli, *Gaussian interference networks: sum capacity in the low-interference regime and new outer bounds on the capacity region*, IEEE Transactions on Information Theory **55** (2009), no. 7, 3032–3050.
3. Salman Beigi, Sida Liu, Chandra Nair, and Mehdi Yazdanpanah, *Some results on the scalar gaussian interference channel*, Proc. IEEE International Symposium on Information Theory (ISIT), 2016, pp. 2199–2203.
4. A. Carleial, *A case where interference does not reduce capacity (corresp.)*, IEEE Transactions on Information Theory **21** (1975), no. 5, 569–570.
5. _____, *Interference channels*, IEEE Transactions on Information Theory **24** (1978), no. 1, 60–70.
6. Max H. M. Costa, *On the Gaussian interference channel*, IEEE Transactions on Information Theory **31** (1985), no. 5, 607–615.
7. _____, *Noisebergs in Z Gaussian interference channels*, Proc. Information Theory and Applications Workshop (ITA), 2011, pp. 1–6.
8. _____, *A third critical point in the achievable region of the z-Gaussian interference channel*, Information Theory and Applications Workshop (ITA), 2014.
9. Max H. M. Costa, Amin Gohari, Chandra Nair, and David Ng, *A proof of the noiseberg conjecture for the Gaussian z-interference channel*, 2023 IEEE International Symposium on Information Theory (ISIT), 2023, pp. 1824–1829.
10. Max H. M. Costa and Chandra Nair, *On the achievable rate sum for symmetric Gaussian interference channels*, Proc. Information Theory and Applications Workshop (ITA), 2012.
11. _____, *Phase transitions in the achievable sum-rate of symmetric Gaussian interference channels*, Proc. Inf. Theory Appl. Workshop, 2013, pp. 10–15.
12. _____, *Gaussian Z-interference channel: around the corner*, Proc. Information Theory and Applications Workshop (ITA), 2016, pp. 1–6.
13. Max H. M. Costa, Chandra Nair, and David Ng, *On the Gaussian Z-interference channel*, Proc. Information Theory and Applications Workshop (ITA), 2017, pp. 1–15.
14. Max H. M. Costa, Chandra Nair, David Ng, and Yan Nan Wang, *On the structure of certain non-convex functionals and the Gaussian Z-interference channel*, Proc. IEEE International Symposium on Information Theory (ISIT), 2020, pp. 1522–1527.
15. Raul H. Etkin, David N. C. Tse, and Hua Wang, *Gaussian interference channel capacity to within one bit*, IEEE Transactions on Information Theory **54** (2008), no. 12, 5534–5562.
16. Amin Gohari and Chandra Nair, *Outer bounds for multiuser settings: the auxiliary receiver approach*, IEEE Transactions on Information Theory **68** (2022), no. 2, 701–736.
17. Amin Gohari, Chandra Nair, and David Ng, *An information inequality motivated by the Gaussian Z-interference channel*, Proc. IEEE International Symposium on Information Theory (ISIT), 2021.
18. Amin Gohari, Chandra Nair, and Jinpei Zhao, *On the capacity region of some classes of interference channels*, 2024 IEEE International Symposium on Information Theory (ISIT), 2024, pp. 3136–3141.
19. Te Sun Han and Kingo Kobayashi, *A new achievable rate region for the interference channel*, IEEE Transactions on Information Theory **27** (1981), no. 1, 49–60.
20. G. Kramer, *Outer bounds on the capacity of gaussian interference channels*, IEEE Transactions on Information Theory **50** (2004), no. 3, 581–586.
21. _____, *Review of rate regions for interference channels*, 2006 International Zurich Seminar on Communications, 2006, pp. 162–165.
22. Omar Mehanna, John Marcos, and Nihar Jindal, *On achievable rates of the two-user symmetric gaussian interference channel*, 2010 48th Annual Allerton Conference on Communication, Control, and Computing (Allerton), 2010, pp. 1273–1279.
23. Abolfazl Seyed Motahari and Amir Keyvan Khandani, *Capacity bounds for the Gaussian interference channel*, IEEE Transactions on Information Theory **55** (2009), no. 2, 620–643.
24. Wai Ho Ng, *On Gaussian extremizers for the capacity region of the Gaussian interference channel*, Ph.D. thesis, The Chinese University of Hong Kong (Hong Kong), 2021.
25. Yury Polyanskiy and Yihong Wu, *Wasserstein continuity of entropy and outer bounds for interference channels*, CoRR **abs/1504.04419** (2015).
26. _____, *Wasserstein continuity of entropy and outer bounds for interference channels*, IEEE Transactions on Information Theory **62** (2016), no. 7, 3992–4002.
27. I. Sason, *On achievable rate regions for the Gaussian interference channel*, IEEE Transactions on Information Theory **50** (2004), no. 6, 1345–1356.
28. _____, *On the corner points of the capacity region of a two-user Gaussian interference channel*, IEEE Transactions on Information Theory **61** (2015), no. 7, 3682–3697.

29. H. Sato, *Two-user communication channels*, IEEE Transactions on Information Theory **23** (1977), no. 3, 295–304.

30. _____, *On degraded gaussian two-user channels (corresp.)*, IEEE Transactions on Information Theory **24** (1978), no. 5, 637–640.

31. _____, *The capacity of the Gaussian interference channel under strong interference (corresp.)*, IEEE Transactions on Information Theory **27** (1981), no. 6, 786–788.

32. Xiaohu Shang, Gerhard Kramer, and Biao Chen, *A new outer bound and the noisy-interference sum-rate capacity for Gaussian interference channels*, IEEE Transactions on Information Theory **55** (2009), no. 2, 689–699.